Journal Pre-proof

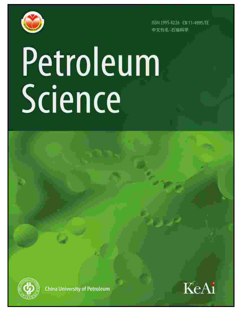

Driving forces and their relative contributions to hydrocarbon expulsion from deep source rocks: A case of the Cambrian source rocks in the Tarim Basin

Bo Pang, Junqing Chen, Xiongqi Pang, Tao Hu, Yue Sheng

PII: S1995-8226(22)00190-X

DOI: https://doi.org/10.1016/j.petsci.2022.08.011

Reference: PETSCI 306

To appear in: *Petroleum Science*

Received Date: 19 October 2021

Revised Date: 26 May 2022

Accepted Date: 11 August 2022

Please cite this article as: Pang, B., Chen, J., Pang, X., Hu, T., Sheng, Y., Driving forces and their relative contributions to hydrocarbon expulsion from deep source rocks: A case of the Cambrian source rocks in the Tarim Basin, *Petroleum Science* (2022), doi: https://doi.org/10.1016/j.petsci.2022.08.011.

Driving Forces and their Relative Contributions to Hydrocarbon Expulsion from Deep Source Rocks: A Case of the Cambrian Source Rocks in the Tarim Basin

Bo Pang[1,2], Junqing Chen[1,3,4,5]*, Xiongqi Pang[1,2]*, Tao Hu[1,2], Yue Sheng[6]

[1] State Key Laboratory of Petroleum Resources and Prospecting, China University of Petroleum, Beijing 102249, China;

[2] College of Geoscience, China University of Petroleum, Beijing 102249, China;

[3] College of Science, China University of Petroleum, Beijing 102249, China;

[4] Laboratory of Optical Detection Technology for Oil and Gas, China University of Petroleum-Beijing, Beijing 102249, China

[5] Basic Research center for Energy Interdisciplinary, China University of Petroleum, Beijing 102249, China;

[6] CNPC Economics & Technology Research Institute, Beijing 100029, China.

*Corresponding Authors: Junqing Chen: chenjq@cup.edu.cn; Xiongqi Pang: pangxq@cup.edu.cn

Abstract: To thoroughly understand the dynamic mechanism of hydrocarbon expulsion from deep source rocks, in this study, five types of hydrocarbon expulsion dynamics (thermal expansion, hydrocarbon diffusion, compaction, product volume expansion, and capillary pressure difference (CPD)) are studied. A model is proposed herein to evaluate the relative contribution of different dynamics for hydrocarbon expulsion using the principle of mass balance, and the model has been applied to the Cambrian source rocks in the Tarim Basin. The evaluation results show that during hydrocarbon expulsion from the source rocks, the relative contribution of CPD is the largest (>50%), followed by compaction (10%–40%), product volume expansion (5%–30%), and thermal expansion (2%–20%). The relative contribution of diffusion to hydrocarbon expulsion is minimal (<10%). These results demonstrate that CPD plays an important role in the hydrocarbon expulsion process of deep source rocks. The hydrocarbon expulsion process of source rocks can be categorized into three stages based on the contribution of different dynamics to the process: the first stage is dominated by compaction and diffusion to expel hydrocarbons, the second stage is dominated by product volume expansion and CPD, and the third stage is dominated by product volume expansion and CPD. This research offers new insights into hydrocarbon exploration in tight oil and gas

reservoirs.

Keywords: Driving force; Dynamic mechanism; Hydrocarbon expulsion; Deep oil and gas exploration; Tarim Basin

1. Introduction

Tight oil and gas reservoirs are widely distributed in the deep tight reservoirs, accounting for more than 85% of the total unconventional oil/gas resources (Zou 2014; Jia 2017; Tong et al. 2018). Their great resource potential has attracted considerable attention from petroleum geologists and explorers for a long time (SPE et al. 2007; Jarvie 2012; Jia 2017; Zheng et al. 2019)**Error! Reference source not found.**. Tight oil and gas reservoirs have completely different dynamics from those of conventional oil and gas reservoirs; therefore, the distribution of tight oil and gas reservoirs is mainly controlled by source rocks (Zou 2014; Pang et al. 2021b). Considering that deep oil and gas reservoirs are widely distributed in tight reservoirs, most scholars believe that the hydrocarbon migration and accumulation in tight reservoir layers (**Fig. 1**) is driven by nonbuoyancy forces (Zou et al. 2012; Song et al. 2019; Jia et al. 2021)**Error! Reference source not found.**. However, there are various types of nonbuoyancy forces and their effects on hydrocarbon expulsion are different.

Previous studies assumed that overpressure was the main driving force for hydrocarbon expulsion from source rocks (Dickinson 1953; Hunt 1990; Osborne and Swarbrick 1997; Hao 2005; Jiang et al. 2016). However, there are several formation mechanisms of overpressure, including product volume expansion, thermal expansion, and compaction (Hao 2005; Jiang et al. 2016). For evaluating the effect of different dynamics on hydrocarbon expulsion more accurately, the hydrocarbon expulsion dynamics are summarized based on Pang’s (2000; 2001; 2021b) research. According to Pang’s research, there were five types of dynamics and nine driving forces, i.e., compaction due to overlying strata (Lee et al. 2018), product volume expansion due to organic matter transformation (Espitalie et al. 1980) and clay mineral dehydration (Lindgreen 1985), thermal expansion of minerals and fluids (water, oil, and gas) in source rocks (Magara 1975a, 1975b; Baker 1984; Olgaard et al. 1997), diffusion caused by the hydrocarbon concentration gradient (Leythaeuser 1982), and capillary pressure difference (CPD) between surrounding source rocks and inner reservoirs (Magara 1979; Stainforth and Reinders 1990). The importance of these forces in hydrocarbon expulsion has been verified by several scholars (Chen and Tian 1989; Pittman 1992;

Li 2004; Qiao et al. 2019). However, the most important driving force among these nonbuoyancy forces in the process of hydrocarbon expulsion remains unclear. Currently, how to determine the dominant driving force in the process of hydrocarbon expulsion from source rocks is the most crucial problem for geologists.

Numerous studies have evaluated the importance of different hydrocarbon expulsion dynamics (Magara 1979; Espitalie et al. 1980; Leythaeuser 1982; Rose 2001) and mainly focused on a single driving force (Lindgreen 1985; Stainforth and Reinders 1990). However, the study of single driving force cannot effectively reflect the effect of the driving force in the entire hydrocarbon expulsion process, resulting in incomplete understanding of the dynamics in the hydrocarbon expulsion process. Therefore, revealing dominant driving forces and quantitatively evaluating their contributions to hydrocarbon expulsion in deep areas is of practical significance for understanding the main controlling factors of hydrocarbon expulsion. This benefits explorations in tight reservoirs. Based on the abovementioned research purposes, herein, we focus on the differences and correlations of these driving forces in oil/gas expulsion from source rocks to quantify their relative contributions in a tight reservoir formation with increasing depth.

Fig.1. Distribution of deep and tight reservoirs and their relation to buoyancy-driven hydrocarbon accumulation depth (BHAD) (quoted from Pang et al. 2021b). A. Driving force of hydrocarbon migration is changed from buoyancy to nonbuoyancy with increasing depth. B. Distribution of conventional and unconventional oil and gas resources and their relation to BHAD. C. Decreases in the maximum pore throat radius in the target layer result in the transformation of hydrocarbon accumulation dynamic mechanisms from shallow reservoirs to deep and tight reservoirs. BHAD is defined as the critical condition corresponding to the change in the hydrocarbon driving force (Pang et al. 2021b).

2. Geological setting

The Tarim Basin is rich in deep-seated oil and gas resources. Oil and gas are mainly concentrated in Paleozoic marine strata (Han et al. 2012; Zhu et al. 2012; Lan et al. 2015). The lithology of the target strata mainly presents carbonate rocks, including limestone and dolomite (Hu et al. 2015; Liu et al. 2015). The maximum depth of the oil and gas reservoirs is more than 8800 m, and their formation and distribution are mainly related to fault zones, unconformities, and reconstructed reservoirs (**Fig. 2**; Yu et al. 2012; Huang et al. 2015, 2016; Shen et al. 2018). These oil and gas reservoirs are mainly reformed as unconventional tight oil and gas reservoirs distributed near the source rocks (Shen et al. 2018). Therefore, the Tarim Basin is selected as the research object in our study to provide some suggestions for its deep exploration. The Paleozoic Middle–Lower Cambrian and Middle–Upper Ordovician source rocks are realized as the main source rocks in the deep area of the Tarim Basin (Li et al. 2010, 2015; Huang et al. 2015, 2016). The source rocks are mainly developed marine carbonate rocks and mudstones (Shen et al. 2018). In our study, the Cambrian source rocks are the main research objects.

Fig.2. Distribution characteristics of Paleozoic marine crude oil and its correlation with the Ordovician and Cambrian source rocks in the Tazhong Uplift, Tarim Basin. A. Plane distribution characteristics of the oil and gas reservoirs. B. Oil and gas reservoirs section (northwest to southeast). C. Conceptual model of the oil and gas accumulation in the reservoirs of the trending section.

3. Method and parameters

3.1 Classification of driving forces

Previous research works (Pang et al. 2001; Pang et al. 2021b) have studied the five types of dynamics (T1–T5) and nine driving forces (F1–F9) of hydrocarbon expulsion, and sufficient evidence of each driving force has been proposed (Magara 1974; Berg 1975; Magara 1979; Espitalie et al. 1980; Leythaeuser 1982; Lindgreen 1985; Stainforth and Reinders 1990; Rose 2001). **Fig.3** presents the differences between these driving forces in the burial process of the source rocks.

Hydrocarbon diffusion (T1) is regarded as a type of dynamics for hydrocarbon expulsion from source rocks (Leythaeuser 1982; Rose 2001; Qiao et al. 2019), expressed as **F1**. However, the total amount of expelled hydrocarbon is limited because the diffusion coefficient of hydrocarbons through rock media is very small (Leythaeuser 1982).

The thermal expansion (T2) of minerals and fluids is another type of dynamics for hydrocarbon expulsion from source rocks (Olgaard et al. 1997). This type of dynamics can be subdivided into the thermal expansion of mineral skeleton (**F2**), water (**F3**), liquid oil (**F4**), and natural gas (**F5**) (Magara 1975a, 1975b; Baker 1984). The amounts of the expelled fluid or hydrocarbon are mainly related to the total amount of minerals, water, oil, and gas in the source rocks and their thermal expansion coefficients (Magara 1975a, 1975b; Baker 1984). The driving force increases with increasing burial depth and temperature. However, it may be mainly confined to the early and middle stages because the residual pore fluids (water, oil, and gas) in the source rocks are very little in deep strata (Magara 1975a). In addition, the amount of hydrocarbon expelled due to mineral expansion is very limited because the thermal expansion coefficients of minerals are quite small (Baker 1984).

The compaction of source rocks (T3) by overlying strata is also regarded as a type of dynamics for hydrocarbon migration (Magara 1979; Lee et al. 2018), expressed as **F6**. As the porosity decreases because of compaction, the residual hydrocarbon saturation in the pores increases and free phase hydrocarbon is discharged in large quantities (Chen et al. 1989). The compaction may be mainly confined to the early stage of hydrocarbon expulsion in argillaceous source rocks and may not be as important in the middle and late stages with greater burial depth (Lee et al. 2018). In addition, its significance for hydrocarbon expulsion in the water-soluble phase may be greater than that in the other phase states. However, the amount of hydrocarbons expelled via compaction is very limited because the solubility of oil and gas in water is small (Price 1976).

Product volume expansion (T4) through organic-parent-material pyrolysis transformation (Espitalie et al. 1980) and clay mineral dehydration (Magara 1975a; Lindgreen 1985) is regarded as the fourth type of dynamics for hydrocarbon expulsion, expressed as kerogen transformation to oil/gas (**F7**) and clay dehydration (**F8**). During the burial of source rocks, several material transformations result in an increase in volume, generating energy for discharging oil and gas (England et al. 1987). These transformations mainly occur in the middle stage of hydrocarbon expulsion from source rocks. However, their contribution to hydrocarbon expulsion in source rocks may be very limited owing to the small expansion coefficient (Espitalie et al. 1980; Lindgreen 1985).

The CPD (T5) between the source rocks and the adjacent reservoirs is regarded as the fifth type of dynamics for hydrocarbon expulsion from source rocks (Berg 1975), expressed as **F9**. Capillary forces have been considered as the resistance to hydrocarbon migration for a long time (Hubbert 1953; Pittman 1992). In 1987, England put forward the concept of interfacial potential (England et al. 1987), and scholars began to consider the CPD between source rocks and the surrounding rocks as the driving force for hydrocarbon migration (Berg RR 1975; Dickey 1975; Du 1981; Pang et al. 2021b). However, the contribution of CPD remains controversial (Rouchet 1981;

Stainforth and Reinders 1990)Error! Reference source not found.. Some researchers believe that the effect of CPD on hydrocarbon migration and accumulation is very limited and should be neglected because of its small value (Dickey 1975; Du 1981; Li 2004; Bao et al. 2017)Error! Reference source not found.. Some believe that although CPD plays a very important role, it is limited to certain geological conditions in the evolution of source rocks when massive hydrocarbons are generated and organic networks are formed in a source rock (McAulife 1979; England et al. 1987; Jia et al. 2020)Error! Reference source not found.. Further, the contribution of CPD is considered to be confined in reservoirs with highly uneven pore structure characteristics, where oil and gas constantly migrate from small capillary pores to larger pores, leading to gradual oil and gas enrichment (Zou et al. 2012; Jiang et al. 2017; Pang et al. 2021a; Jia et al. 2021).

Fig.3. Driving forces for hydrocarbon expulsion from the source rocks and variation characteristics of the hydrocarbon expulsion amount under the action of each type of force with increasing depth.

3.2 Simulation method

Previous studies have proven that each of the aforementioned five types of dynamics and nine driving forces (Pang et al. 2001; Pang et al. 2021) can lead to hydrocarbon expulsion from source rocks. However, various complicated phenomena can be involved in the process of hydrocarbon expulsion (Magara 1974; Berg 1975; Magara 1979; Espitalie et al. 1980; Leythaeuser 1982; Lindgreen 1985; Stainforth and Reinders 1990; Rose 2001), implying that the five types of dynamics and nine driving forces of hydrocarbon expulsion can all simultaneously exist but make different contributions at different stages. On the basis of the principle of material balance, the relative contributions of the nine forces are determined via numerical simulations using the following five steps (**Fig.4**).

The first step is to study the evolution history of petroliferous basins and calculate the amount of hydrocarbon generation, retention, and expulsion from source rocks (Pang et al. 2016)Error! Reference source not found..

The second step is to estimate the amount of hydrocarbon expulsion from the following four phases of source rocks and their changing histories (Johnson 1912). The oil/gas amounts expelled (Q_e) from source rocks in the water-soluble phase (Q_{ew}) (Price 1977)Error! Reference source not found., diffusion phase (Q_{ed}) (Leythaeuser et al. 1982; Thomas and Clouse 1990)Error! Reference source not found., oil-soluble phase (Q_{eog}) (Neglia 1979),**Error! Reference source not found.** and free phase (Q_{es}) (Dickey 1975)**Error! Reference source not found.** are hereby studied.

The third step is to study the oil/gas expulsion mechanisms of the nine driving forces and calculate the fluid volume (ΔQ_f, f = 1, 2,…,9) expelled from the source rocks by each driving force.

The fourth step is to calculate the amount of hydrocarbon (Q_{ef}, f = 1, 2,…, 9) expelled via the nine driving forces according to their expelled fluid volumes and relationships to oil/gas amounts expelled from the four phases. The amount of hydrocarbon expelled in the diffusion phase (Q_{ed}) was only related to F1 and that involved in the water-soluble phase (Q_{ew}) was associated with F2–F8. The amounts of hydrocarbons in the oil-solution phase (Q_{eo}) and the free phase (Q_{es}) are contributed by F2–F9. The total expelled hydrocarbon quantity (Q_{ef}) for all driving forces is the sum of the oil/gas amount expelled in the four phases, which could be denoted as $Q_{ef} = Q_{edf} + Q_{ewf} + Q_{eof} + Q_{esf}$, f = 1, 2, 3, …, 9.

The fifth step is to evaluate the relative contribution (Kf) of each driving force (f) to all the oil/gas amounts expelled from source rocks in different phases during a certain depth interval, denoted as $Kf = Qef/\sum(Qeif)$, f = 1, 2, …9. The value of $\sum(Qei)$ refers to the sum of the cumulative hydrocarbon amounts expelled by the nine driving forces in the four phases. The variations in Qef and Kf with the increasing burial depth of source rocks were calculated at 250-m depth intervals.

Fig.4. Technologies for evaluating the contributions of nine driving forces to oil/gas expulsion from source rocks and their workflow.

F1 is the diffusion force for hydrocarbon expulsion from source rocks. F2–F5 are the thermal expansion forces of mineral skeleton, water, liquid oil, and natural gas. F6 is the compaction stress from overlying strata. F7 and F8 occur due to pressures from increasing fluid volumes caused by clay dehydrates and kerogen transformation to oil/gas. F9 is the CPD between the source rocks and the surrounding rocks. ΔQ_{f2}–ΔQ_{f8} are the fluid volumes expelled by driving forces F2–F8. Q_{ef1}–Q_{ef9} are the oil/gas amounts expelled by driving forces F1–F9. K_j is the relative contributions of each driving force Fj, j = 1, 2, …, 9.

3.2.1 Simulation of hydrocarbon expulsion amounts from source rocks

The following numerical simulation is based on the recovery of the burial history and thermal evolution of the source rocks, and relevant methods can be found in previous studies (Lerche 1990; Pang et al. 1993; Pang et al. 2001).

The generated hydrocarbon's amount depends on the quality and maturity of the source rocks. According to the principle of mass balance, the generated hydrocarbon amount (Q_p) per cubic meter of source rock (Pang et al., 1993, 2001) is denoted as follows:

$$Q_p = R_p(R_o, KTI) \cdot D(z) \cdot TOC(R_o, KTI)/100, \tag{1}$$

where Q_p is the total amount of hydrocarbon generated per cubic meter of source rock (in kg/m^3 for oil and m^3/m^3 for gas), $R_p(R_o, KTI)$ refers to the hydrocarbon amount generated per unit weight of organic matter (in kg/t for oil and in m^3/t for gas), whose quantitative relationship has already been established (Tissot and Welte 1978; Hunt 1979), $D(Z)$ is the source-rock density (t/m^3), which varies with depth (Z) (Magara et al. 1981), and TOC is the original total organic carbon content (%). The generated hydrocarbon components are divided into three groups: liquid oil (C_n, $n \geq 6$), heavy hydrocarbon gas ($C_{2\text{–}5}$), and methane gas (C_1).

The calculation model of the total residual oil amount is modified based on the report by Pang (2001) and expressed as Equ. (2):

$$Q_{ro} = \rho_o \cdot (\varphi_n + \Delta\varphi) \cdot (A_0 + A_1 \cdot (TOC) + A_2 \cdot (TOC)) \cdot \frac{1}{1\text{-}B_k} \cdot e^{-\frac{\varphi_n}{D}(R_o - R')^2}, \tag{2}$$

where Q_{ro} refers to the total amount of residual oil per cubic meter of source rock (kg/m^3), φ_n is the porosity of source rocks with normal compaction (%), and $\Delta\varphi$ is the extra porosity of source rocks with abnormal compaction (%). R_o refers to the critical vitrinite reflectance corresponding to the maximum value of the residual hydrocarbon peak (%). ρ_o denotes the crude oil density (t/m^3). A_0, A_1, A_2, and D denote the constant values determined through statistical analysis (Behar et al. 2001) with the best fitness between the actual data "S_1" or "A" with the calculation model (Pang et al. 2001). B_k is the light-hydrocarbon compensation factor (Chen et al. 2018), which is quantitatively related to major factors established before (Pang et al. 1993).

The total residual gas amount in the source rocks can be divided into three types and calculated using Equ. (3):

$$Q_{rg} = (Q_{rgb} + Q_{rgo} + Q_{rgw} + Q_{rs}), \tag{3}$$

where Q_{rg} is the total amount of residual gas per cubic meter of source rock (m^3/m^3), including the adsorbed gas amount of Q_{rgb} (Qu et al. 2020), oil-dissolved gas amount of Q_{rgo} (He et al. 2020), water-dissolved gas amount of Q_{rgw} (Li et al. 2018), and free gas amount of Q_{rs} (Rexer et al. 2013).

Similarly, according to the principle of material balance, the amount of hydrocarbon expulsion from source rocks in different phases can be calculated (Pang et al. 2001) using Equ. (4):

$$Q_e = R_e(R_o, KTI) \cdot D(z) \cdot TOC(R_o, KTI)/100, \quad (4)$$

where Q_e is the total hydrocarbon expulsion amount per cubic meter of source rock (in kg/m^3 for oil and in m^3/m^3 for gas) and $R_e(R_o, KTI)$ is the amount of hydrocarbon expelled per unit weight of organic matter (in kg/t for oil and in m^3/t for gas), which changes with KTI and R_o (Pang et al. 2005; Jiang et al. 2016).

The hydrocarbon expulsion threshold (HET) of the source rocks can be determined using Equ. (5), which corresponds to the critical conditions (Pang et al. 2020; Pang et al. 2021a) where the generated hydrocarbon amount (Q_p) is equal to the residual hydrocarbon amount (Q_{rm}):

$$Q_p \geq Q_{rm} = Q_{ro} + Q_{rg}. \quad (5)$$

3.2.2 Simulation of hydrocarbon expulsion from source rocks in different phases

The phase states of the oil and gas expelled from source rocks can be mainly divided into four phases: the diffusion phase (Price 1977), water-soluble phase (Leythaeuser et al. 1982), oil-soluble phase (Neglia 1979), and free phase (Dickey 1975).

The amount of hydrocarbon expelled from source rocks in the water-soluble phase can be calculated (Leythaeuser et al. 1982) using Equ. (6):

$$Q_{ew} = V_{ew} \cdot \sum_1^4 q_{ew}(i), \quad (6)$$

where Q_{ew} is the amount of hydrocarbon expelled as a water-soluble (in kg/m^3 for oil and in m^3/m^3 for gas), changing with the water volume expelled from source rocks (V_{ew}), hydrocarbon component (i), and hydrocarbon solubility in water (q_{ew}). q_{ew} is controlled by the oil/gas component (i), temperature (T), pressure (P), and water mineralization (X_k), and their relationships can be confirmed (Price et al. 1977).

The amount of hydrocarbon expelled from source rocks in the diffusion phase can be calculated (Price 1977) using Equ. (7):

$$Q_{ed} = \sum_1^4 \int_0^t D(i,T,\emptyset) \cdot \frac{d_c}{d_z} \cdot d_t, \quad (7)$$

where Q_{ed} refers to the amount of hydrocarbon expelled as the diffusion phase (in kg/m^3 for oil) and in m^3/m^3 for gas), changing with the source-rock distribution areas (S), diffusion time (t), inside hydrocarbon composition (i), concentration gradient (dc/dz), and diffusion coefficient D (i, T, Φ). The relationships of the diffusion coefficient with hydrocarbon components (i), temperature (T), and medium porosity (Φ) are determined (Leythaeuser et al. 1982).

The amount of hydrocarbon expelled from source rocks as an oil-solution phase can be calculated (Neglia 1979) using Equ. (8).

$$Q_{eog}=Q_{eo}\cdot\sum_{1}^{4}q_o(i), \tag{8}$$

where Q_{eog} denotes the amount of gas expelled from source rocks as an oil-solution phase (in kg/m^3 for oil and in m^3/m^3 for gas), changing with the amount of expelled oil and the solubility of the gas in the oil (q_{o}). The relationships of q_{o} and the gas component (i), temperature (T), pressure (P), and oil density (ρ_{o}) were determined by Bruce (1984).

The amount of hydrocarbon expelled from source rocks in the free phase can be calculated (Dickey 1975) using Equ. (9):

$$Q_{es}=Q_e-Q_{\mathrm{ew}}-Q_{\mathrm{ed}}-Q_{\mathrm{eog}}, \tag{9}$$

where Q_{es} is the amount of hydrocarbon expelled in the free phase (in kg/m^3 for oil and in m^3/m^3 for gas), changing with the total hydrocarbon expulsion amount from the source rocks ($Q_{\mathrm{p}}-Q_{\mathrm{rm}}$). The hydrocarbon expulsion amount from the source rocks in the free phase is most significant for oil/gas accumulation (Magara et al. 1978).

Further, the characteristics of hydrocarbon expulsion from source rocks during the evolution of source rock can be analyzed. These characteristics can be expressed as the following parameters: velocity (V_{e}), rate (S_{e}), and efficiency (R_{e}) of hydrocarbon expulsion and the source-rock index (*SRI*). These key parameters for hydrocarbon expulsion at different depth intervals are calculated using Equ. (10)–(13):

$$V_e=\frac{\Delta Q_e}{\Delta Z}, \tag{10}$$

$$S_e=\frac{\Delta Q_e}{H}, \tag{11}$$

$$R_e=\frac{Q_e}{Q_P}, \text{ and} \tag{12}$$

$$SRI=\frac{Q_{es}}{Q_e}, \tag{13}$$

where V_e is the hydrocarbon expulsion velocity, changing with ΔQ_{e} and depth, S_{e} is the hydrocarbon expulsion rate, changing with V_{e} and the thickness of the source rocks (H), and R_e is the hydrocarbon expulsion efficiency, changing with different depths of the source rocks. *SRI* changes with the total oil/gas amount expelled from source rocks in the free phase (Q_{es}) and the total oil/gas amount expelled in different phases (Q_e).

3.2.3 Simulation of the relative contribution of different dynamics to hydrocarbon expulsion

The amount of hydrocarbon expelled in the diffusion phase (Q_{ed}) is controlled by the driving force F1. The hydrocarbon amount expelled from source rocks in the water-soluble phase (Q_{ew}) is controlled by the combination of seven driving forces (F_i, i = 2–8). Furthermore, the oil/gas amounts expelled in the oil-solution (Q_{eog}) and free (Q_{es}) phases are related to these eight driving forces (F_i, i = 2–9). The volumes of the liquid expelled from the source rocks due to different dynamics were calculated first to compare the relative magnitudes of various hydrocarbon expulsion dynamics.

The liquid volume expelled from source rocks owing to different driving forces can be calculated as follows (Pang et al. 2001). The volumes of the fluids expelled by seven driving forces are denoted as $\triangle V_{fi}$, i = 2, 3,…, 8.

The volumes of the liquid expelled by thermal expansion can be calculated using Equ. (14)–(17) (Pang et al. 2001; 2003).

$$V_{f2}=(K_{sr2}-K_{sr1})\cdot(1\text{-}\Phi_0), \quad (14)$$

$$V_{f3}=(K_{hw2}-K_{hw1})\cdot\left(\frac{\varphi_0-\varphi_2}{1-\varphi_2}-\frac{\varphi_0-\varphi_1}{1-\varphi_1}\right), \quad (15)$$

$$V_{f4}=(K_{ho2}-K_{ho1})\cdot\left(\frac{\varphi_0-\varphi_2}{1-\varphi_2}-\frac{\varphi_0-\varphi_1}{1-\varphi_1}\right)\cdot S_o, \text{ and} \quad (16),$$

$$V_{f5}=(K_{hg2}-K_{hg1})\cdot\left(\frac{\varphi_0-\varphi_2}{1-\varphi_2}-\frac{\varphi_0-\varphi_1}{1-\varphi_1}\right)\cdot S_G, \quad (17),$$

where $\triangle V_{f2}$ is the volume of liquid expelled via the thermal expansion of mineral skeleton. K_{sr} is related to the expansion coefficient of the skeleton content ($1-\Phi_0$) (David et al. 1997). $\triangle V_{f3}$ is the volume of liquid expelled via the thermal expansion of water, which is related to the source-rock porosity (Φ) and water expansion coefficient (K_{hw}) (Barker 1980). ΔV_{f4} is the volume of liquid expelled via the thermal expansion of oil, which is related to the source-rock porosity (Φ), oil expansion coefficient (K_{ho}), and oil saturation (S_o) in source rocks (Magara 1976). $\triangle V_{f5}$ is the volume of liquid expelled via the thermal expansion of gas, which is related to the variation of the source-rock porosity (Φ) and the gas-expansion coefficient (K_{hg}) (Magara 1976).

The volumes of liquid expelled via compaction can be calculated using Equ. (18) (Pang et al. 2001; 2003).

$$V_{f6}=\left(\frac{\varphi_0-\varphi_2}{1-\varphi_2}-\frac{\varphi_0-\varphi_1}{1-\varphi_1}\right)\cdot H, \quad (18)$$

where ΔV_{f6} is the volume of liquid expelled via compaction and is related to porosity (Φ) and thickness of source rock (H) (Lee et al. 2018).

The volumes of liquid expelled via product volume expansion can be calculated using Equations (19) and (20) (Pang et al. 2001; 2003).

$$V_{f7}=(D_1-D_2)\cdot(TOC_2-TOC_1)\cdot K_v \text{ and} \tag{19}$$

$$V_{f8}=0.245\cdot(C_{lay2}-C_{lay1})\cdot(I_{m2}-I_{m1})\cdot(D_2-D_1), \tag{20}$$

where ΔV_{f7} is the volume of liquid expelled via kerogen transformation, which is related to TOC, the density of source rocks (D), and the volume-increase coefficient (K_v) (Vernik and Landis 1996). ΔV_{f8} is the volume of liquid expelled via clay dehydration, which is associated with the total content of clay minerals (C_{lay}) and secondary illites (I_m) formed via clay diagenesis and the volume-increase coefficient (England et al. 1987).

According to the volume of liquid expelled from source rocks owing to different dynamics, the relative magnitude of various hydrocarbon expulsion dynamics can be calculated using the modified Darcy's law (Germann 2018) using Equ. (21).

$$F_i=\left[\cdot\frac{\mu H}{KS}\cdot\frac{dV_i}{\cdot d_t}\right]\cdot 10^{12} \quad (i = 2,3,\ldots\ldots,8), \tag{21}$$

where F_i is the relative magnitude of different hydrocarbon expulsion dynamics, μ_i is the fluid viscosity, which is replaced by water viscosity because the water volume is the highest among the expelled fluid volume, accounting for 70% (Zheng et al. 2020), and H, K, and S represent the thickness, permeability, and area of the source rocks, respectively.

The relative magnitude of the ninth driving force (F9) can be calculated (McAulife 1979; England et al. 1987) using Equ. (22) and (23).

$$F_{9o}=Pc_{W/O}=2\cdot\delta_{W/O}\cdot\cos\theta\cdot\left(\frac{1}{r}-\frac{1}{R}\right) \text{ and} \tag{22}$$

$$F_{9g}=Pc_{W/G}=2\cdot\delta_{W/G}\cdot\cos\theta\cdot\left(\frac{1}{r}-\frac{1}{R}\right), \tag{23}$$

where Pc is the CPD between the source and surrounding rocks, r is the throat radius of surrounding rocks, R is the throat radius of reservoirs, and θ is the wetting angle of hydrocarbon/water. The capillary pressure differences between oil (F_{9o}) and gas (F_{9g}) are calculated separately.

According to the relationship between the hydrocarbon expulsion dynamics and the phase state of hydrocarbon expulsion, combined with the relative magnitude of the hydrocarbon expulsion dynamics, the relative contribution of different hydrocarbon expulsion dynamics to the amount of hydrocarbon expulsion was calculated.

The hydrocarbon amount of Q_{ed} expelled via F_1 is denoted as Q_{e1} and calculated (Leythaeuser 1982) using Equ. (24).

$$Q_{e1}=D\cdot\frac{d_C}{d_Z}\cdot\frac{1-\varphi_0}{1-\varphi_2}\cdot s\cdot\varphi_2\cdot\Delta t, \tag{24}$$

where D is the diffusion coefficient, d_C/d_Z is the hydrocarbon concentration gradient, S is the diffusion area, φ is the porosity of the source rocks, and t is the diffusion period.

The amount of hydrocarbon expelled (Q_{ei}) via each of the other eight driving forces is calculated using Equ. (25). Q_{ew} is expelled owing to the combination of $\sum F_i$, i = 2, 3,…, 8, whereas Q_{eog} and Q_{es} are expelled because of the combination of $\sum F$i, i = 2, 3, …, 9.

$$Q_{ei}=(Q_{es}+Q_{eog})/F_i+Q_{ew}/F_j \ \ (j = 2,3,\ldots\ldots,8;\ i = 2,3,\ldots.,9). \tag{25}$$

Finally, the relative contributions of each driving force are obtained using Equ. 26.

$$R_i=\frac{Q_{ei}}{\sum_{i=1}^{9}Q_{ei}} \ \ (i = 2, 3,\ldots\ldots, 8). \tag{26}$$

3.3 Model parameters

The basic parameters of the Cambrian source rocks in the Tarim Basin must be obtained to accurately simulate their hydrocarbon expulsion processes. The source-rock parameters required in the abovementioned simulations mainly include the following five types of data: the thickness of the source rocks (H), total organic carbon (TOC) of the source rocks, kerogen type index (KTI), thermal evolution degree (R_o) or burial depth (Z), and thermal gradient. The characteristics of these parameters are illustrated in **Fig. 5** and **Table 1**. Under the given geological conditions, H ranges from 0 to 450 m, with an average of ~200 m, TOC changes from 0.2% to 3.3%, with an average of 1.5%, KTI changes from 50 to 100, with an average of 85, the equivalent R_o changes from 0.8% to 4.1%, with an average of 1.8%, and the thermal gradient changes from 2.3 to 2.7°C/100 m, with an average of 2.5°C/100 m.

In addition to considering actual geological conditions, studying the amounts of hydrocarbon expulsion under various dynamic effects of source rocks involves a series of calculation parameters. These include the rock heat-expansion coefficient (Magara et al. 1975b), hydrocarbon heat-expansion coefficient (Magara 1975a), hydrocarbon diffusion coefficient (Leythaeuser 1987), natural gas–adsorption coefficient (Danial and Bustin 2007), dissolution coefficient of hydrocarbon in water (Price 1976), dissolution coefficient of gas in oil (Neglia et al. 1979), volume expansion coefficient of kerogen products (Espitalie et al. 1980), and clay mineral dehydration (Dickinson et al. 1953). These parameters used in the abovementioned equations are obtained from previous studies and listed in **Table 2**. Using the obtained geological condition data and parameters, the hydrocarbon expulsion model of the Cambrian source rocks in the Tarim Basin can be established accurately.

Table 1. Geological parameters of the Cambrian source rocks in the Tarim Basin.

Geological Data	Source-rock thickness (m)	Total organic carbon (*TOC*) (%)	Kerogen type index (*KTI*)	Maturity (R_o) (%)	Thermal gradient (°C/100 m)
Maximum	450	0.2	50	0.8	2.7
Minimum	0	3.3	97	4.1	2.3
Mean	200	1.5	85	1.8	2.5
Source	Li et al., 2010, 2015; Shen et al., 2018	Li et al., 2010, 2015; Shen et al., 2018	Pang et al., 1992; Li et al., 2010, 2015	Li et al., 2010, 2015; Shen et al., 2018	Han et al., 2012; Hu et al., 2015; Liu et al., 2015

Table 2. Sources of the driving force parameters.

Driving force parameters		**Sources**
Diffusion coefficient		Leythaeuser et al., 1982
Thermal expansion coefficients	Rock	Magara et al., 1975b
	Water	Barker, 1980
	Liquid oil	Magara, 1975a
	Natural gas	Magara, 1975a
Volume expansion coefficient	Kerogen products	Espitalie et al., 1980
	Clay mineral dehydration	Dickinson et al., 1953
Natural gas–adsorption coefficient		Danial et al., 2007
Hydrocarbon dissolution coefficient in water		Price, 1976
Gas dissolution coefficient in oil		Neglia et al., 1979

Fig.5. Distribution characteristics of the geochemical and geological parameters of the Cambrian source rocks in the Tarim Basin. A. Total organic carbon (%). B. Organic-parent-material type (*KTI*). C. Organic maturity degree of the equivalent vitrinite reflectance (%). D. Thickness of source rocks (m).

4. Results

4.1 Hydrocarbon expulsion in four phases from source rocks

Fig.6 illustrates the case study results of hydrocarbon expulsion from the source rocks of the Tarim Basin in four different phases. **Fig.6A** shows the variation characteristics of hydrocarbon generation, retention, and expulsion with increasing depth for methane (**A1**); heavy gas (**A2**); liquid hydrocarbons (**A3**); and *SRI* (**A4**), clarifying the relationship of the generated, retained, and expelled oil/gas amounts per cubic meter in the evolution of source rocks. **Fig.6B** shows the variation characteristics of hydrocarbon expulsion per cubic meter of source rocks with increasing depth. The oil/gas expulsion is characterized by four parameters: the accumulatively expelled hydrocarbon amount (**B1**), hydrocarbon expulsion velocity (**B2**), hydrocarbon expulsion rate per 100-m-depth-interval increase (**B3**), and oil/gas expulsion efficiency (**B4**). **Fig.6C** shows the variation of relative amounts (%) of hydrocarbon expelled from source rocks in the four phases at the same depth intervals, including those for methane gas, heavy hydrocarbon gas, and liquid hydrocarbon.

Fig.6. Case study of the numerical simulation results on hydrocarbon generation, retention, and expulsion in four different phases for the source rocks in the Tarim Basin with the following essential parameters: TOC = 1.5%, KTI = 85, R_o = 1.8%, H = 200 m, GT = 2.5°C/100 m. A. Variations of hydrocarbon generation, retention, and expulsion per cubic meter of source rocks with increasing depth for methane (A1), heavy hydrocarbon gas (A2), liquid (A3), and source-rock index (*SRI*). B. Variation of the hydrocarbon expulsion characteristics of the hydrocarbon expulsion amount (B1), hydrocarbon expulsion velocity rate (B2), hydrocarbon expulsion rate (B3), and hydrocarbon expulsion efficiency (B4). C. Variations of the relative oil/gas amounts expelled in four different phases from source rocks, including methane (C1), heavy gas (C2), and liquid hydrocarbons (C3). *W*, *D*, *O*, and *F* represent the relative amounts of hydrocarbons expelled from the source rocks in the water-soluble, diffusion, oil-solution, and free phases, respectively.

4.2 Relative contributions of the nine driving forces to oil/gas expulsion

Fig.7 presents the variation characteristics of the total water, natural gas (methane and heavy gas), and liquid oil expelled per cubic meter of source rocks by the nine driving forces with increasing depth. **Fig.7A** shows the variation characteristics of the expelled water amount, expressed as instantaneous amounts per 100-m-depth intervals (**A1**), relative amounts (**A2**), and cumulative amounts (**A3**). **Fig.7B** shows the variation characteristics of the expelled gas amount, expressed as instantaneous amounts per 100-m-depth intervals (**B1**), relative amounts (**B2**), and cumulative amounts (**B3**). **Fig.7C** shows the variation characteristics of the expelled liquid-oil amounts expressed as instantaneous amounts (**C1**), relative amounts (**C2**), and cumulative amounts (**C3**). The total amount of water expelled from the source rocks is mainly related to compaction (50%), clay dehydration (35%), the thermal expansion of rock skeleton and fluids (9%), and kerogen transformation (6%). Compaction (F6) made the largest contribution to water expulsion, whereas CPD made the largest contribution to gas expulsion (>80%). Meanwhile, the contribution of diffusion was ~5%, while those of clay dehydration and kerogen transformation was 5% in total, and the compaction (4%) and thermal expansion of rock skeleton and fluids (<5%) had the smallest contributions. The contributions of the nine driving forces to the expelled oil amount were almost the same as the contributions to the expelled gas amount, which was mainly dominated by CPD (>85%), compaction (7%), clay and kerogen transformation (5%), and the thermal expansion of rock skeleton and fluids (<3%). As shown by the numerous simulation results obtained using various geological parameters, the contribution of CPD to the total expelled oil/gas amount was more than 50% with TOC > 0.5% and R_o > 0.5%, and its relative contribution increased with increasing depth. This implies CPD's dominant role in the formation and distribution of deep and tight oil/gas reservoirs.

Fig.7. Numerical simulation results for the fluid expulsion of water, oil, and gas due to the nine driving forces from the source rocks and their relative contributions with increasing burial depth. A. Variation characteristics of the expelled liquid amounts from the source rocks, including instantaneous expelled liquid amounts (A1), relative expelled liquid amounts (A2), and accumulative expelled liquid amounts (A3). B. Variation characteristics of the expelled gas amount, including instantaneous expelled gas amounts (B1), relative expelled gas amounts (B2), and accumulative expelled gas amounts (B3). C. Variation characteristics of the expelled oil amount, including instantaneous expelled oil amounts (C1), relative expelled oil amounts (C2), and accumulative expelled oil amounts (C3). F1 denotes the diffusion of hydrocarbons. F2–F5 denote the thermal volume expansions of mineral skeleton, water, liquid oil, and natural gas. F6 denotes the compaction caused by overlying strata. F7 and F8 denote the product volume expansions induced via clay dehydration and kerogen transformation to oil/gas. F9 denotes the capillary pressure difference (CPD).

4.3 Dynamic model for oil/gas expulsion from source rocks with increasing depth

The dynamic process of hydrocarbon expulsion from source rocks is divided into four stages with increasing depth, showing that different forces expel hydrocarbons from source rocks in different phases at different stages and make different contributions to oil and gas accumulations in deep and tight reservoirs (**Fig.8**).

Fig.8. Dynamic model for hydrocarbon expulsion in four phases from source rocks and the stage division based on the variation characteristics of the driving forces' contributions with increasing depth. The F_s definitions are the same as those presented in **Fig.7**.

The first stage is from the deposition of source rocks at the beginning to the HET underground, dominated by the compaction of overburdened strata. Most of the oil and gas were expelled in water-soluble and diffusion phases, and the relative contributions of compaction (F6), diffusion (F1), thermal expansion (F2–F5), and product volume expansion (F7–F8) are approximately 40%, 25%, 20%, and 15%, respectively. This is unfavorable for oil/gas migration and accumulation in reservoir layers because the generated oil/gas amounts are insufficient to accomplish the retention of oil and gas in source rocks and oil/gas could not be expelled massively in the free phase. The accumulative expelled oil/gas amounts in this stage is less than 10% of the total amount, primarily because of the low solubility of oil/gas in water, the small diffusion coefficient of oil/gas through the rocks, and the very limited oil and gas amounts generated by the source rocks.

The second stage is from HET to the liquid hydrocarbon expulsion depth (LHED), where both oil and gas were expelled from the source rocks in four phases. Most (65%–85%) oil and gas were expelled in the free phase (with some gas migrating in the oil-solution phase), dominated by multidriving forces, i.e., CPD, thermal expansion, and product volume expansion, and others. Their relative contributions to oil/gas expulsion are 40%, 30%, 20%, and 10%, respectively. The source-rock distribution area with developed sapropel-type organic parent material is conducive to the formation of pure oil reservoirs where natural gas is dissolved. The source-rock distribution area with developed humic-type organic parent material is favorable for the formation of pure gas reservoirs. Meanwhile, the distribution of source rocks with transitional-type organic parent material is favorable for the formation of oil and gas reservoirs.

The third stage begins with source rocks entering LHED and lasts to the active source-rock depth limit, indicating the end of hydrocarbon generation and expulsion (Pang et al. 2020). Natural gas with little liquid oil is expelled from the source rocks in the free phase. More than 50% of the natural gas is expelled in this stage via CPD, and the relative hydrocarbon amounts expelled through diffusion, thermal expansion of rocks and fluids, and compaction of overlying strata are less than 5%, 10%, and 15%, respectively.

In summary, CPD is the most important driving force for hydrocarbon expulsion from effective source rocks. Its relative contribution is more than 50% with a porosity of <10% ± 2%, which increases with increasing depth. Meanwhile, the other eight driving forces are important for hydrocarbon expulsion but are limited by the evolution stage of source rocks and the phases of the expelled hydrocarbons. Their total contributions to hydrocarbon expulsion are less than 50%. These results imply that the deeper the source rocks, the more important CPD becomes for tight hydrocarbon reservoir accumulation.

5. Discussion

For a long time, overpressure has been considered the main driving force for hydrocarbon expulsion from source rocks (Dickinson 1953; Hunt 1990; Osborne and Swarbrick 1997; Hao 2005; Jiang YL et al. 2016). During the formation and evolution of sedimentary basins, many physical and chemical processes can produce overpressure (Holbrook et al. 1995; Tingay et al. 2009). It is generally believed that the main reasons for large-scale overpressure in sedimentary basins are compaction, fluid expansion and kerogen conversion (Hao 2005; Jiang YL et al. 2016). However, the hydrocarbon expulsion of source rocks is controlled by complicated geological factors, and their contributions to hydrocarbon expulsion at different stages vary greatly. Therefore, it is necessary to establish a unified model to study the dynamics of hydrocarbon expulsion in the process of hydrocarbon expulsion from source rocks. In this study, a model for evaluating the contribution of multiple dynamics to hydrocarbon expulsion was established and applied to the Cambrian source rocks in the Tarim Basin. The results demonstrate that CPD is the most important contributor to hydrocarbon expulsion in tight reservoirs, especially in the deep formation. This may be related to the four characteristics of CPD: (1) always coexists between source rocks and surrounding reservoir layers due to the difference in their pore throat (Pang et al. 2021a); (2) is continuously and uninterruptedly active (Jia et al. 2021); (3) irreversible migration direction from smaller to larger throats (England 1987); and (4) irreplaceable role in the accumulation of oil/gas in deep and tight reservoirs where the effects of other driving forces greatly weaken and almost disappear (Magara 1987)[Error! Reference source not found.].

It should be noted that the result of the model changes due to different geological conditions. Most hydrocarbons are generated in source rocks and primarily accumulate in source rocks to form shale oil or gas resources (Liu et al. 2017). However, in the Tarim Basin, fractures and secondary pores generated by tectonic movement improve the quality of the reservoirs, increasing the pore throat radius in the reservoirs and generating large CPD (Pang et al 2016). And the exploration results in the Tarim Basin demonstrate that 92% of the proven reserves are distributed in the deep tight reservoirs developed with fractures and secondary pores (**Fig.9**; Shen et al. 2018), where there exists large CPD between the source rocks and surrounding rocks. The exploration results confirm the reliability of this model. However, when source rocks are in contact with reservoirs with low porosity and permeability, the CPD makes a relatively small contribution to hydrocarbon expulsion. Therefore, in order to better understand the dynamic mechanism of hydrocarbon expulsion of source rocks in different basins, it is necessary to establish models for different source rocks. In addition, some parameters in this model are obtained from laboratory conditions, which may have slight errors compared with the parameters in the geological conditions.

Fig.9. Distribution characteristics of the proven reserves of oil and gas in the Tarim Basin. A. The vertical distribution indicates that 92% of the proven oil and gas reserves are in deep and tight reservoirs with depths of >4500 m. B. Favorable exploration areas include three types: complex structures in the foreland basin, deep carbonate rocks, and lithologic and stratigraphic reservoirs in the platform basin. All the discovered oil and gas reservoirs and 95% of the proven reserves are distributed in the favorable exploration area.

6. Conclusions

1. Continuous tight oil/gas reservoirs are widely developed in deep petroliferous basins, and the main dynamics associated with the oil/gas expulsion from source rocks can be divided into five types (and nine driving forces). Under the combined action of various dynamics, hydrocarbons are expelled from the source rocks in four phases. Based on the principle of material balance, a numerical model is proposed in this study to evaluate the relative contribution of different dynamics for hydrocarbon expulsion from the source rocks. The model can obtain the relative contribution of each dynamic on hydrocarbon expulsion in the geological history.

2. This numerical model is applied to the Cambrian source rocks in the Tarim Basin. Among the driving forces, the simulation results demonstrate that the CPD is the most important driving force for hydrocarbon expulsion in the Cambrian source rocks, expelling a large amount of

hydrocarbons in the free phase. The contributions of compaction, product volume expansion, and thermal expansion to hydrocarbon expulsion are relatively small. The relative contribution of diffusion to the expulsion of hydrocarbons is the smallest, mainly expelling hydrocarbons in the diffusion phase.

3. The process of hydrocarbon expulsion can be divided into three stages. The first stage is when hydrocarbons are expelled via compaction and diffusion in the water-soluble and diffusion phases, which is not beneficial for oil and gas accumulation. The second stage features a large amount of hydrocarbon expulsion, and it expels hydrocarbons in various phases via CPD and product volume expansion. The third stage is when gas is expelled in the free phase due to volume thermal expansion and CPD. The second and third stages are the most important stages of hydrocarbon expulsion from the source rocks.

Acknowledgements

This study is financially supported by the Joint Fund of the National Natural Science Foundation of China under grant number U19B6003-02-04, the Science Foundation of China University of Petroleum, Beijing, under grant number 2462020BJRC005 and 2462022YXZZ007, and the National Natural Science Foundation of China under grant number 42102145. We highly appreciate the leaders and experts of the Tarim Oilfield Company, PetroChina, as well as the scientists from our research group. Further, we are grateful to Xinhe Shao, Kun Zhang, and Wenyang Wang, who contributed immensely to improving this manuscript.

Reference

Bao YS, Zhang LY, Zhang SC, et al. Effectiveness of Capillary Pressure on the Primary Migration of Oil and Its Accumulation. Geological Journal of China Universities. 2017; 23(02): 296-303. DOI: 10.16108/j.issn1006-7493.2016211 (in Chinese)

Barker C. Primary migration: the importance of water-mineral-organic matter interactions in the source rock. AAPG Bull. 1980; 34: 1-19. DOI: 10.1306/St10411C2

Behar F, Beaumont V, De B, et al. Rock-Eval 6 Technology: Performances and Developments. Oil & Gas Science & Technology. 2001; 56(2): 111-134. DOI: 10.2516/OGST:2001013.

Berg RR. Capillary pressures in stratigraphic traps. *AAPG bulletin*. 1975; 59(6):939-956. DOI: 10.1306/83D91EF7-16C7-11D7-8645000102C1865D.

Bruce C. Smectite dehydration; its relation to structural development and hydrocarbon accumulation in northern gulf of mexico basin. AAPG Bull. 1984; 68(6): 673-683. DOI: 10.1007/BF01081374.

Chen FJ and Tian SC. Compaction and oil and gas migration. China University of Geoscience Press. 1989.

Chen J, Pang X, Pang H. et al. Hydrocarbon evaporative loss evaluation of lacustrine shale oil based on mass balance method: Permian Lucaogou Formation in Jimusaer Depression, Junggar Basin. Mar and Petro Geo. 2018; 191: 422-431. DOI: 10.1016/j.marpetgeo.2018.01.021.

Danial J and Bustin R. Impact of mass balance calculations on adsorption capacities in microporous shale gas reservoirs. Fuel. 2007; 86(17-18): 2696-2706. DOI: 10.1016/j.fuel.2007.02.036.

David L, Janos U, Lisa N, et al. The influence of swelling clays on the deformation of mudrocks. Int J Rock Mech Min. 1997; 34(3-4): 364-364. DOI: 10.1016/S0148-9062(97)00224-6.

Dickey PA. Possible Primary Migration of Oil from Source Rock in Oil Phase. AAPG Bulletin. 1975; 59(2): 337-345. DOI: 10.1306/83D91C8B-16C7-11D7-8645000102C1865D.

Dickinson G. Geological aspects of abnormal reservoir pressures in Gulf Coast Louisiana. AAPG Bulletin. 1953; 37(8): 410-432. DOI: 10.1306/5CEADC6B-16BB-11D7-8645000102C1865D.

Du R. Stress fields: a key to oil migration. AAPG Bull. 1981; 65(1): 168-174. DOI: 10.1306/2F919774-16CE-11D7-8645000102C1865D.

Duvall F, Hong YS, Pitt CH. Physical behavior of oil shale at various temperatures and compressive loads: 2. Thermal expansion under various loads. Fuel. 2015; 64(2): 184-188. DOI: 10.1016/0016-2361(85)90214-5.

England W, Mackenzie A, Mann D, et al. The movement and entrapment of petroleum fluids in the subsurface. J Geol Soc London. 1987; 144: 327-347. DOI: 10.1144/gsjgs.144.2.0327.

Espitalie J, Madec M, Tissot B. Role of mineral matrix in kerogen pyrolysis; influence on petroleum generation and migration. AAPG Bull. 1980; 64(1): 59-66. DOI: 10.1007/BF01081857.

Germann P. Viscosity-The weak link between Darcy's law and Richards' capillary flow. Hydrol Processes. 2018; 32(9): 1166-1120. DOI: 10.1002/hyp.11450.

Ghaderi SM, Clarkson CR, Kaviani D. Investigation of primary recovery in tight oil formations: A look at the Cardium Formation, Alberta. Canadian Unconventional Resources Conference. Society of Petroleum Engineers, 2011. DOI: 10.2118/148995-MS

Han JF, Zhang HZ, Yu HF, et al. Hydrocarbon accumulation characteristic and exploration on large marine carbonate condensate field in Tazhong Uplift. Acta Petrol. Sin. 2012; 28(3): 769–782. DOI:CNKI:SUN:YSXB.0.2012-03-007 (in Chinese).

Hao F. Kinetics of hydrocarbon generation and mechanisms of petroleum accumulation in overpressure basins. Beijing: Science Press. 2005 (in Chinese).

He X, Gui Y, Xie J. et al. A DFT study of dissolved gas (C2H2, H2, CH4) detection in oil on CuO-modified BNNT. Appl Surf Sci. 2020; 500:144030. DOI: 10.1016/j.apsusc.2019.144030.

Holbrook PW, Maggiori DA, Hensley R. Real-time pore pressure and fracture gradient evaluation in all sedimentary lithologies. SPE Formation Evaluation. 1995; 10(4): 215-222. DOI: 10.2118/26791-PA.

Hu ZY, Sun D, Hu YY, et al. The controlling effect of carbonate fault system on reservoirs: a case study in the 3rd block of Tazhong area. Natural Gas Geoscience. 2015; 26, 97-106. DOI: 10.11764/j.issn.1672-1926.2015.S1.009.

Huang HP, Zhang SC, Su J. Palaeozoic oil–source correlation in the Tarim Basin, NW China: a review. Org. Geochem. 2016; 94, 32–46. DOI: 10.1016/j.orggeochem.2016.01.008

HUBBERT MK. Entrapment of petroleum under hydrodynamic conditions. AAPG Bulletin. 1953; 37(8): 1954-2026. DOI: 10.1306/5CEADD61-16BB-11D7-8645000102C1865D.

Hunt JM. Generation and migration of petroleum from abnormally pressured fluid compartments. AAPG Bulletin. 1990; 74(1): 1-12. DOI: 10.1029/JB095iB01p00649.

Hunt JM. Petroleum Geochemistry and Geology (lst edition). New York: W. H. Freeman and Company, 1979.

JARVIE DM. Shale resource systems for oil and gas: Part 2: Shale-oil resource systems. BREYER J A. Shale reservoirs: Giant resources for the 21st century. Tulsa: AAPG, 2012: 89-119.

Jia CZ, Pang XQ, Song Y. The mechanism of unconventional hydrocarbon formation: Hydrocarbon self-sealing and intermolecular forces. Petroleum Exploration and Development. 2021; 48(3):507-526. DOI: 10.1016/S1876-3804(21)60042-3.

JIA CZ. On the breakthrough of unconventional oil and gas to classical oil and gas geology theory and its significance. Petroleum Exploration and Development. 2017; 44(1): 1-11. DOI: 10.1016/S1876-3804(17)30002-2

Jiang F, Pang X, Bai J, et al. Comprehensive assessment of source rocks in the Bohai Sea area, eastern China. AAPG Bull. 2016; 100(6): 969-1002. DOI: 10.1306/02101613092

Jiang H, Pang XQ, Yu R, et al. Lower limit of hydrocarbon accumulation in the Kuqa Depression, Tarim Basin, NW China. Geological Journal. 2017; 52: 141-153. DOI: 10.1002/gj.2740.

Jiang YL, Wang X, Yu QQ, et al. Pressure field characteristics of petroliferous depressions and its relationship with hydrocarbon enrichment in Bohai Bay Basin. Acta Petrol Sin. 2016; 37(11): 1361-1369. DOI: 10.7623/syxb201611004 (in Chinese).

Johnson RH. The Accumulation of Oil and Gas in Sandstone. *Science*. 1912; Mar 22;35(899): 458-9. DOI: 10.1126/science.35.899.458.

Kilk, K., Savest, N., Yanchilin, A., et al. Solvent swelling of dictyonema oil shale: low temperature heat-treatment caused changes in swelling extent. Journal of Analytical and Applied Pyrolysis, 2010, 89(2): 261-264. DOI: 10.1016/j.jaap.2010.09.003.

Lan XD, Lv XX, Zhu YM. The geometry and origin of strike-slip faults cutting the Tazhong low rise megaanticline (central uplift, Tarim Basin, China) and their control on hydrocarbon distribution in carbonate reservoirs. J. Nat. Gas Sci. Eng. 2015, 22, 633–645. DOI: 10.1016/j.jngse.2014.12.030.

Law BE. Basin-centered gas systems. AAPG Bulletin, 2002, 86(11): 1891–1919. DOI: 10.1306/61EEDDB4-173E-11D7-8645000102C1865D.

Lee W, Kang P, Kim A, et al. Impact of surface porosity on water flux and structural parameter in forward osmosis. Desalination. 2018; 439: 46-57. DOI: 10.1016/j.desal.2018.03.027

Lerche I. Basin Analysis: Quantitative Methods. San Diego: Academic Press, 1990.

Leythaeuser D, Mackenzie A, Schaefer R, et al. A novel approach for recognition and quantification of hydrocarbon migration effects in shale-sandstone sequences. AAPG Bull. 1984; 68(2): 196-219. DOI: 10.1002/esp.3290080607

Leythaeuser D, Schaefer RG, Yukler A. Role of diffusion in primary migration of hydrocarbons. AAPG bulletin. 1982; 66(4):408-429. DOI: 10.1007/BF01081377

Li C, Zhen K, Hao Y, et al. Effect of dissolved gases in natural water on the flotation behavior of coal. Fuel. 2018; 233(DEC.1): 604-609. DOI: 10.1016/j.fuel.2018.06.104

Li MC. Migration of oil and natural gas. Petroleum Industry Press, 2004 (in Chinese).

Li Q, Pang X, Chen J. Original TOC recovery of hydrocarbon source rock and effective quantitative evaluation for deep carbonate formation in central Tarim basin. Unconventional Oil and Gas.

2016; 03(04): 48-57. DOI: CNKI:SUN:FCYQ.0.2016-04-007 (in Chinese).

Li SM, Amrani A, Pang XQ. Origin and quantitative source assessment of deep oils in the Tazhong Uplift, Tarim Basin. Organic Geochemistry. 2015; 78: 1–22. DOI: 10.1016/j.orggeochem.2014.10.004

Li SM, Pang XQ, Jin ZJ, et al. Petroleum source in the Tazhong Uplift, Tarim Basin: New insights from geochemical and fluid inclusion data. Organic Geochemistry. 2010; 41: 531–553. DOI: 10.1016/j.orggeochem.2010.02.018

Lindgreen H. Diagenesis and primary migration in upper Jurassic claystone source rocks in Northsea. Aapg Bull. 1985; 69(4): 525-536. DOI: 10.1306/ad462524-16f7-11d7-8645000102c1865d.

Liu WB, Ju ZX, Han JF. Hydrocarbon accumulation characteristics and enrichment law of various carbonate layer series of the Ordovician system in III-zone, central Tarim Basin. Natural Gas Geoscience. 2015; 1: 125–137. DOI: 10.11764/j.issn.1672-1926.2015.S2.0125.

Liu YK, Xiong YQ, Li Y, et al. Effects of oil expulsion and pressure on nanopore development in highly mature shale: Evidence from a pyrolysis study of the Eocene Maoming oil shale, south China. Marine and Petroleum Geology. 2017; 86: 526–536. DOI: 10.1016/j.marpetgeo.2017.06.012

Liu Z, Sun Y, Guo W, et al. Reservoir-scale study of oil shale hydration swelling and thermal expansion after hydraulic fracturing. Journal of Petroleum Science and Engineering. 2020; 195:107619. DOI: 10.1016/j.petrol.2020.107619

Lu S, Chen F, Li J. Identification of the lower limit of high-quality source rocks and its relation to hydrocarbon accumulation-taking the Beier Sag in the Hailaer Basin as an example. Petro Sci. 2012; 09(1): 10-17. DOI: 10.1007/s12182-012-0176-y.

Magara K. Compaction and fluid migration. Amsterdam: Elsevier, 1987.

Magara K. Importance of aquathermal pressuring effect in Gulf Coast. AAPG Bull. 1975b; 59(10): 2037-2045. DOI: 10.1306/83D921DB-16C7-11D7-8645000102C1865D.

Magara K. Mechanisms of nature fracturing in a sedimentary basin. AAPG Bull. 1981; 65(1): 123-132. DOI: 10.1306/2F919783-16CE-11D7-8645000102C1865D.

Magara K. Reevaluation of montmorillonite dehydration as cause of abnormal pressure and hydrocarbon migration. *AAPG Bull*. 1975a; 59(2):292-302. DOI: 10.1007/BF01134160.

Magara K. The significance of the expulsion of water in oil-phase primary migration. Bulletin of Canadian Petroleum Geology. 1978.

Magara K. Thickness of removed sediments paleopore pressure and paleotemperature south western part of western Canada Basin. AAPG Bull. 1976; 60: 554-565. DOI: 10.1306/83D92401-16C7-11D7-8645000102C1865D.

McAulife CD. Oil/gas migration-Chemical and physical constraints. AAPG Bull. 1979; 63(5): 767-781. DOI: 10.1306/2f9182cf-16ce-11d7-8645000102c1865d.

Meng WG, Chen ZY, Li P, et al. Exploration theories and practices of buried-hill reservoirs: A case from Liaohe Depression. Petroleum Exploration and Development. 2009; 36(2): 136-143. DOI: 10.1016/S1876-3804(09)60116-6.

Neglia S. Migration of fluids in sedimentary basins. AAPG Bull. 1979; 63(4): 573-597. DOI: 10.1306/2f918194-16ce-11d7-8645000102c1865d.

Olgaard DL, Urai J, Dell'Angelo LN, et al. The influence of swelling clays on the deformation of mudrocks. International Journal of Rock Mechanics & Mining Sciences. 1997; 34(3-4), 364-364. DOI: 10.1016/S0148-9062(97)00224-6.

Osborne MJ and Swarbrick RE. Mechanisms for generating overpressure in sedimentary basins: a reevaluation. AAPG Bull. 1997; 81(6): 1023-1041. DOI: 10.1093/ietcom/e90-b.2.425.

Pang X, Chen Z, Chen F. Study on numerical simulation of geological history, thermal history, hydrocarbon generation-expulsion history and quantitative evaluation of hydrocarbon source rocks in petroliferous basins. Beijing: Geological Publishing House. 1993 (in Chinese).

Pang X, Chen Z, Chen F. The optimum modelling of the amount of oil/gases formed by the kerogens in their evolution based on the material balance principle. Petroleum Exploration and Development. 1992; (01): 23-31. DOI: CNKI:SUN:SKYK.0.1992-01-003 (in Chinese).

Pang X, Li M, Li S. et al. Geochemistry of petroleum systems in the Niuzhuang South Slope of Bohai Bay Basin: Part 3. Estimating hydrocarbon expulsion from the Shahejie formation. Org Geochem. 2005; 36(4): 497-510. DOI: 10.1016/j.orggeochem.2004.12.001.

Pang X, Shao X, Li M, et al. Correlation and difference between conventional and unconventional reservoirs and their unified genetic classification. Gondwana Research. 2021b; 97(6). DOI: 10.1016/j.gr.2021.04.011.

Pang X. Modeling of Geological Processes. Beijing: Petroleum Industry Press. 2003 (in Chinese).

Pang XQ, Chen JQ, Li SM, et al. Evaluation method and application of the relative contribution of marine hydrocarbon source rocks in the Tarim Basin: A case study from the Tazhong area. *Marine & Petroleum Geology*. 2016; 77: 1-18. DOI: 10.1016/j.marpetgeo.2016.05.023.

Pang XQ, Jia CZ, Wang WY, et al. Buoyance-driven Hydrocarbon Accumulation Depth and Its Implication for Unconventional Resource Prediction. **Geoscience Frontiers**. 2021a; 12(4): 101133. DOI: 10.1016/j.gsf.2020.11.019.

Pang XQ, Jia CZ, Zhang K, et al. The dead line for oil and gas and implication for fossil resource prediction. Earth System Science Data. 2020; 12: 577-590. DOI: 10.5194/essd-12-577-2020.

Pang XQ, Jin ZJ, Jiang ZX, et al. Critical Condition for Gas Accumulation in The Deep Basin Trap And Physical Modeling. Natural Gas Geoscience. 2003; 14(3):207-214. DOI: 10.3969/j.issn.1672-1926.2003.03.011 (in Chinese).

Pang XQ, Jin ZJ, Zuo SJ. Dynamics, models and classification of hydrocarbon accumulation. Earth Science Frontiers. 2000; (04):507-514. DOI: 10.3321/j.issn:1005-2321.2000.04.020.

Pang XQ, Lerche I, Wang YC, et al. Theoretical research and application of hydrocarbon expulsion threshold for coal-measure source rocks. Beijing: Petroleum Industry Press. 2001 (in Chinese).

Pang XQ, Liu KY, Ma ZZ, et al. Dynamic field division of hydrocarbon migration, accumulation and hydrocarbon enrichment rules in sedimentary basins. Acta Geologica Sinica. 2012; 86: 1559-1592. DOI: 10.1111/1755-6724.12023.

Pittman ED. Relationship of porosity and permeability to various parameters derived from mercury injection-capillary pressure curves for sandstone. AAPG Bull. 1992; 76: 191-198. DOI: 10.1306/BDFF87A4-1718-11D7-8645000102C1865D.

Price L. Aqueous solubility of petroleum as applied to its origin and primary migration. AAPG Bull. 1976; 60(2): 213-244. DOI: 10.1306/83d922a8-16c7-11d7-8645000102c1865d.

Qi LX. Characteristics and inspiration of ultra-deep fault-karst reservoir in the Shunbei area of the Tarim Basin. China Petroleum Exploration. 2020; 25(01): 102-111. DOI: 10.3969/j.issn.1672-7703.2020.01.010 (in Chinese).

Qiao J, Zeng J, Jiang S, et al. Heterogeneity of reservoir quality and gas accumulation in tight sandstone reservoirs revealed by pore structure characterization and physical simulation. *Fuel*. 2019; 253: 1300–16. DOI: 10.1016/j.fuel.2019.05.112.

Qu Z, Yin Y, Wang H, et al. Pore-scale investigation on coupled diffusion mechanisms of free and adsorbed gases in nanoporous organic matter. Fuel. 2020; 260:116423. DOI: 10.1016/j.fuel.2019.116423.

Rexer TFT, Benham MJ, Aplin AC, et al. Methane adsorption on shale under simulated geological temperature and pressure conditions. Energy & Fuels. 2013; 27(6): 3099-3109. DOI: 10.1021/ef400381v.

Rose W. Modeling forced versus spontaneous capillary imbibition processes commonly occurring in porous sediments. *Journal of Petroleum Science and Engineering*. 2001; 30(3-4): 155-166. DOI: 10.1016/S0920-4105(01)00111-5.

Rouchet JD. Stress Fields, A Key to Oil Migration. Aapg Bull. 1981; 65(1): 74-85. DOI: 10.1306/2F919774-16CE-11D7-8645000102C1865D.

Schmoker JW. Resource-assessment perspectives for unconventional gas systems. AAPG Bull. 2002; 86(11): 1993-1999. DOI: 10.1306/61EEDDDC-173E-11D7-8645000102C1865D.

Shen W, Chen J, Wang Y, et al. The origin, migration and accumulation of the Ordovician gas in the Tazhong III region, Tarim Basin, NW China. Marine & Petroleum Geology. 2018; 101: 55-77. DOI: 10.1016/j.marpetgeo.2018.11.031.

Song Y, Ma XS, Liu SB, et al. Reservoir formation conditions and key technologies for exploration and development of Qinshui coalbed methane field. Acta Petrolei Sinica. 2019; 40(5): 621-634. DOI: 10.7623/syxb201905012 (in Chinese).

SPE, AAPG, WPC, et al. Petroleum resources management system. Washington DC: IEA, 2007.

Stainforth JG and Reinders JEA. Primary migration of hydrocarbons by diffusion through organic matter networks, and its effect on oil and gas generation. Organic Geochemistry. 1990; 16(1-3): 61-74. DOI: 10.1016/0146-6380(90)90026-V.

Teige GMG, Hermanrud C, Wensaas L, et al. The lack of relationship between overpressure and porosity in North Sea and Haltenbanken shales. Marine and Petroleum Geology. 1999; 16(4): 321-335. DOI: 10.1016/S0264-8172(98)00035-X.

Thomas MM and Clouse JA. Primary migration by diffusion through kerogen: II. Hydrocarbon diffusivities in kerogen. *Geochim Cosmochim Acta.* 1990; 54: 2781–2792. DOI: 10.1016/0016-7037(90)90012-A.

Tingay MRP, Hillis RR, Swarbrick RE, et al. Origin for overpressure generation by kerogen-to-gas maturation in the northern Malay Basin. AAPG Bull. 2013; 97(4): 639-672. DOI: 10.1306/09041212032.

Tissot B and Welte D. Petroleum formation and occurrence. Berlin: Springer-Verlag, 1978.

Tong XG, Zhang GY, Wang ZM, et al. Potential and distribution of global oil and gas resources. Petroleum Exploration and Development. 2018; 45(04): 727-736. DOI: 10.11698/PED.2018.04.19.

Vernik L and Landis C. Elastic Anisotropy of Source Rocks: Implications for Hydrocarbon Generation and Primary Migration1. AAPG Bull. 1996; 80(4):531-544. DOI: 10.1306/64ed8836-1724-11d7-8645000102c1865d.

Wang T. Deep basin gas in China. Beijing. Beijing: Petroleum Industry Press. 2002 (in Chinese).

Wu HY, Wang YW, Liang XD, et al. Theory of petroleum accumulation in syncline and its significance to petroleum geology. Earth Science Frontier. 2015; 22(1): 181-188. DOI: 10.13745/j.esf.2015.01.015.

Yu S, Pan CC, Wang JJ, et al. Correlation of crude oils and oil components from reservoirs and source rocks using carbon isotopic compositions of individual nalkanes in the Tazhong and Tabei Uplift of the Tarim Basin, China. Org. Geochem. 2012; 52, 67–80. DOI: 10.1016/j.orggeochem.2012.09.002.

Zhang K, Song Y, Jia CZ, et al. Vertical sealing mechanism of shale and its roof and floor and effect on shale gas accumulation, a case study of marine shale in Sichuan basin, the Upper Yangtze area. Journal of Petroleum Science and Engineering. 2019; 175: 743–754. DOI: 10.1016/j.petrol.2019.01.009.

Zheng D, Pang X, Zhou L, et al. Critical conditions of tight oil charging and determination of the lower limits of petrophysical properties for effective tight reservoirs: A case study from the Fengcheng Formation in the Fengcheng area, Junggar Basin. J of Petro Sci Eng. 2020; 190: 107135. DOI: 10.1016/j.petrol.2020.107135.

Zheng M, Li J, Wu X, et al. Potential of Oil and Natural Gas Resources of Main Hydrocarbon-Bearing Basins and Key Exploration Fields in China. Earth Science. 2019; 44(03): 833-847. DOI: 10.3799/dqkx.2019.957.

Zhu GY, Yang HJ, Su J, et al. New progress of marine hydrocarbon geological theory in China. Acta Petrol. Sin. 2012; 3, 722–738. DOI: 10.2110/palo.2011.p11-036r.

Zou CN, Zhu RK, Wu ST. Conventional and unconventional hydrocarbon accumulations: Taking tight oil and tight gas in China as an instance. Acta Petrolei Sinica. 2012; 33(2): 173-187. DOI: CNKI:SUN:SYXB.0.2012-02-002.

Zou CN. Unconventional Petroleum Geology. Beijing: Geological Publishing House. 2014 (in Chinese).

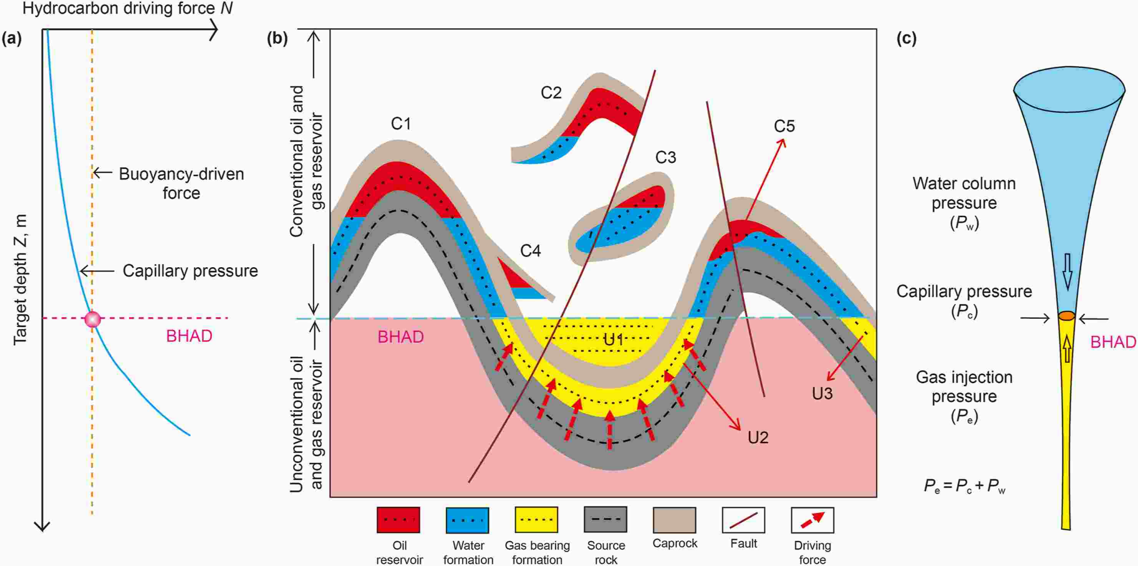

Hydrocarbon driving force N
(a)
Target depth Z, m
Buoyancy-driven force
Capillary pressure
BHAD
(b)
Conventional oil and gas reservoir
Unconventional oil and gas reservoir
C1
C2
C3
C4
C5
BHAD
U1
U2
U3
Oil reservoir
Water formation
Gas bearing formation
Source rock
Caprock
Fault
Driving force
(c)
Water column pressure (P_w)
Capillary pressure (P_c)
BHAD
Gas injection pressure (P_e)
$P_e = P_c + P_w$

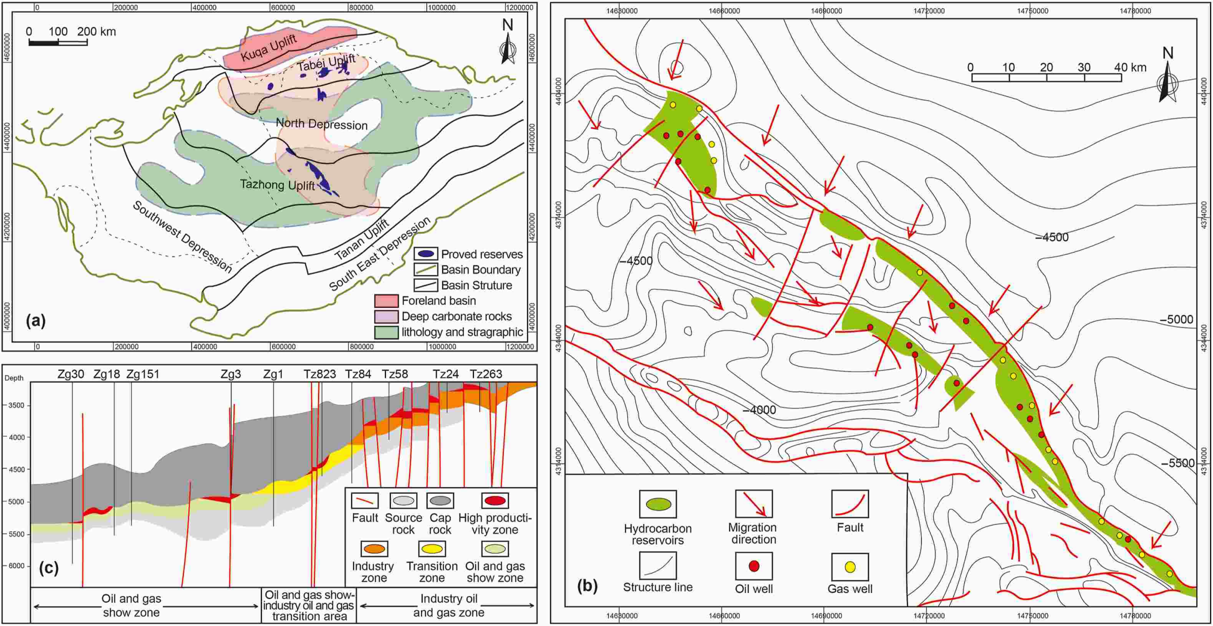

(a)
0 100 200 km
N
Kuqa Uplift
Tabei Uplift
North Depression
Tazhong Uplift
Southwest Depression
Tanan Uplift
South East Depression
Proved reserves
Basin Boundary
Basin Struture
Foreland basin
Deep carbonate rocks
lithology and stragraphic
0
200000
400000
600000
800000
1000000
1200000
4000000
4200000
4400000
4600000
(b)
0 10 20 30 40 km
N
−4500
−4500
−4000
−5000
−5500
14630000
14660000
14690000
14720000
14750000
14780000
4314000
4344000
4374000
4404000
Hydrocarbon reservoirs
Migration direction
Fault
Structure line
Oil well
Gas well
(c)
Depth
3500
4000
4500
5000
5500
6000
Zg30
Zg18
Zg151
Zg3
Zg1
Tz823
Tz84
Tz58
Tz24
Tz263
Fault
Source rock
Cap rock
High productivity zone
Industry zone
Transition zone
Oil and gas show zone
Oil and gas show zone
Oil and gas show-industry oil and gas transition area
Industry oil and gas zone

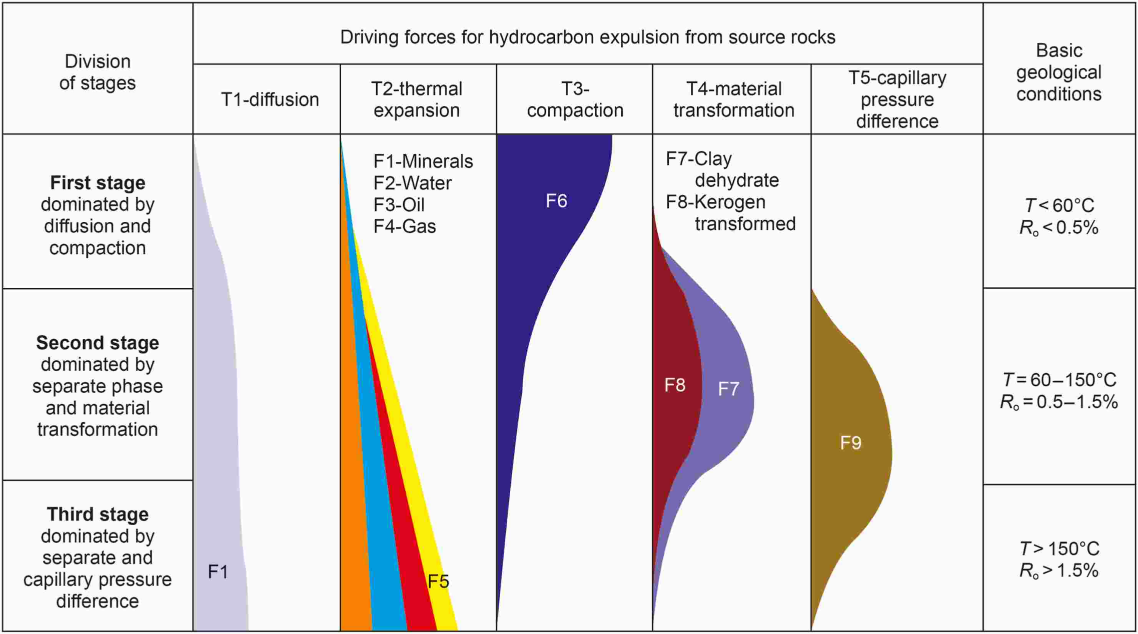

Division of stages
Driving forces for hydrocarbon expulsion from source rocks
T1-diffusion
T2-thermal expansion
T3-compaction
T4-material transformation
T5-capillary pressure difference
Basic geological conditions
First stage dominated by diffusion and compaction
Second stage dominated by separate phase and material transformation
Third stage dominated by separate and capillary pressure difference
F1-Minerals
F2-Water
F3-Oil
F4-Gas
F7-Clay dehydrate
F8-Kerogen transformed
F1
F5
F6
F7
F8
F9
T < 60°C
Ro < 0.5%
T = 60–150°C
Ro = 0.5–1.5%
T > 150°C
Ro > 1.5%

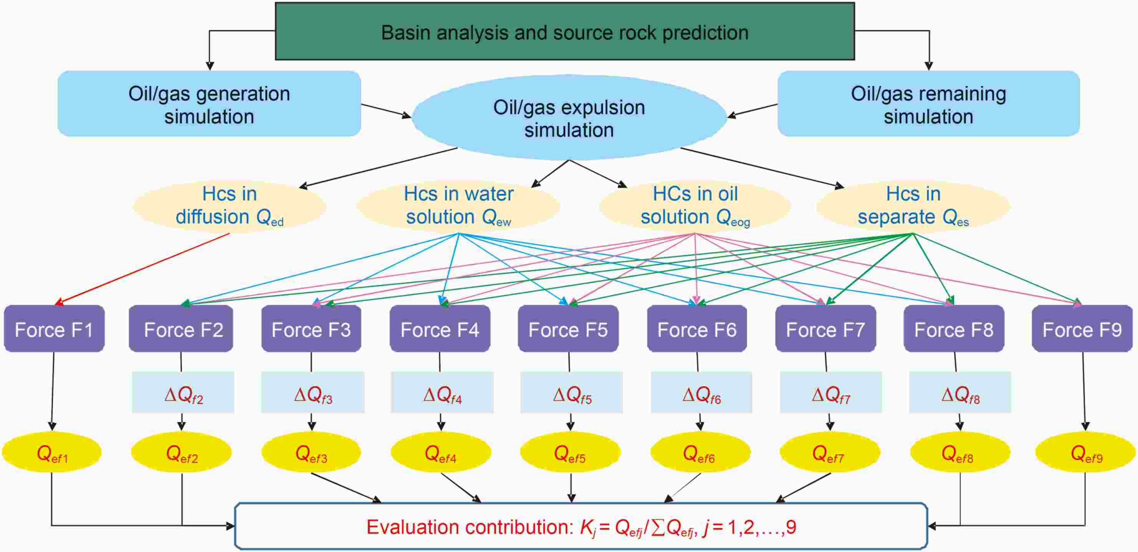

Basin analysis and source rock prediction
Oil/gas generation simulation
Oil/gas expulsion simulation
Oil/gas remaining simulation
Hcs in diffusion Q_{ed}
Hcs in water solution Q_{ew}
HCs in oil solution Q_{eog}
Hcs in separate Q_{es}
Force F1
Force F2
Force F3
Force F4
Force F5
Force F6
Force F7
Force F8
Force F9
ΔQ_{f2}
ΔQ_{f3}
ΔQ_{f4}
ΔQ_{f5}
ΔQ_{f6}
ΔQ_{f7}
ΔQ_{f8}
Q_{ef1}
Q_{ef2}
Q_{ef3}
Q_{ef4}
Q_{ef5}
Q_{ef6}
Q_{ef7}
Q_{ef8}
Q_{ef9}
Evaluation contribution: $K_j = Q_{efj} / \sum Q_{efj}$, $j = 1,2,\ldots,9$

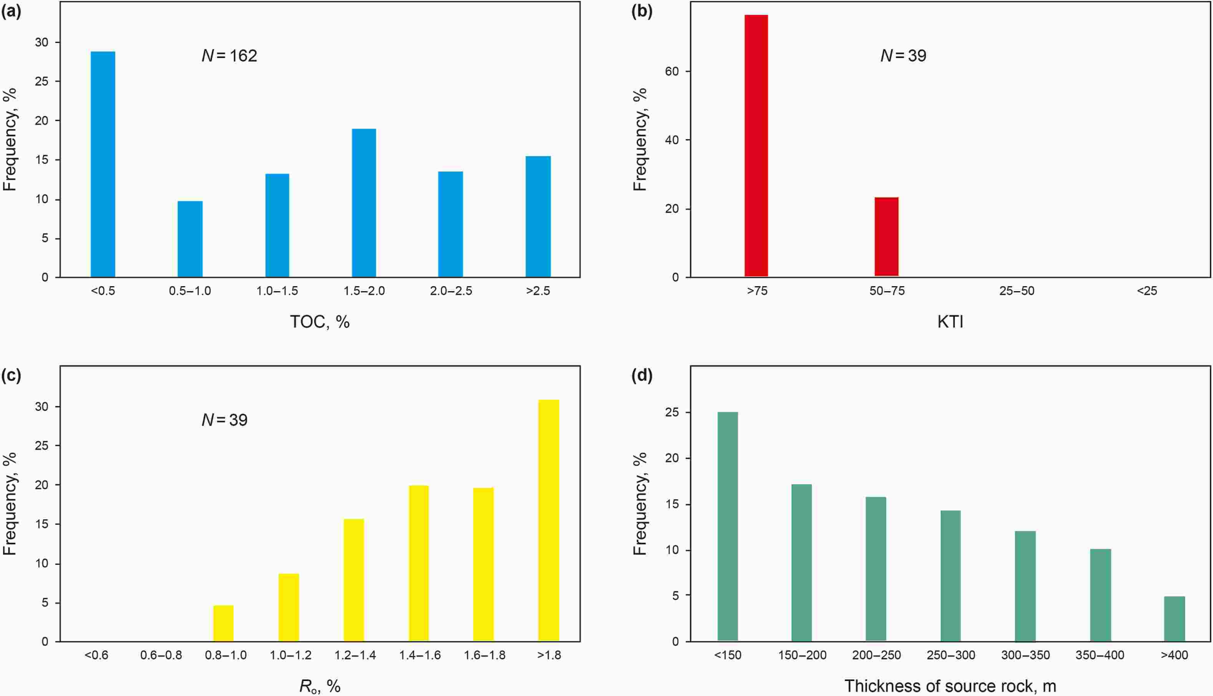

(a)
N = 162
Frequency, %
0
5
10
15
20
25
30
<0.5
0.5–1.0
1.0–1.5
1.5–2.0
2.0–2.5
>2.5
TOC, %
(b)
N = 39
Frequency, %
0
20
40
60
>75
50–75
25–50
<25
KTI
(c)
N = 39
Frequency, %
0
5
10
15
20
25
30
<0.6
0.6–0.8
0.8–1.0
1.0–1.2
1.2–1.4
1.4–1.6
1.6–1.8
>1.8
R_o, %
(d)
Frequency, %
0
5
10
15
20
25
<150
150–200
200–250
250–300
300–350
350–400
>400
Thickness of source rock, m

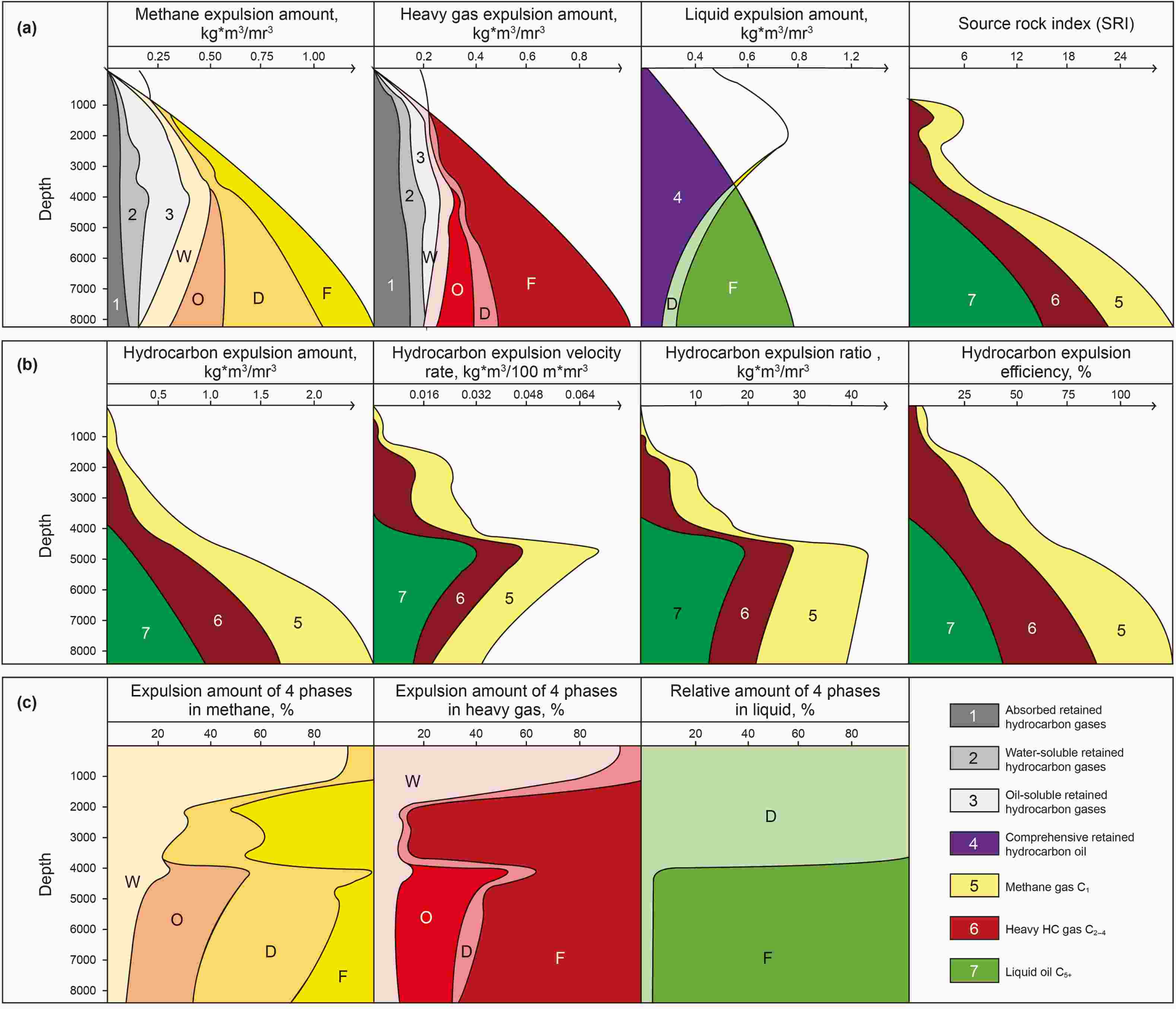

W, D, O, F refer to 4 phases of hydrocarbon expulsion in water-solution, diffusion, oil-solution and in free

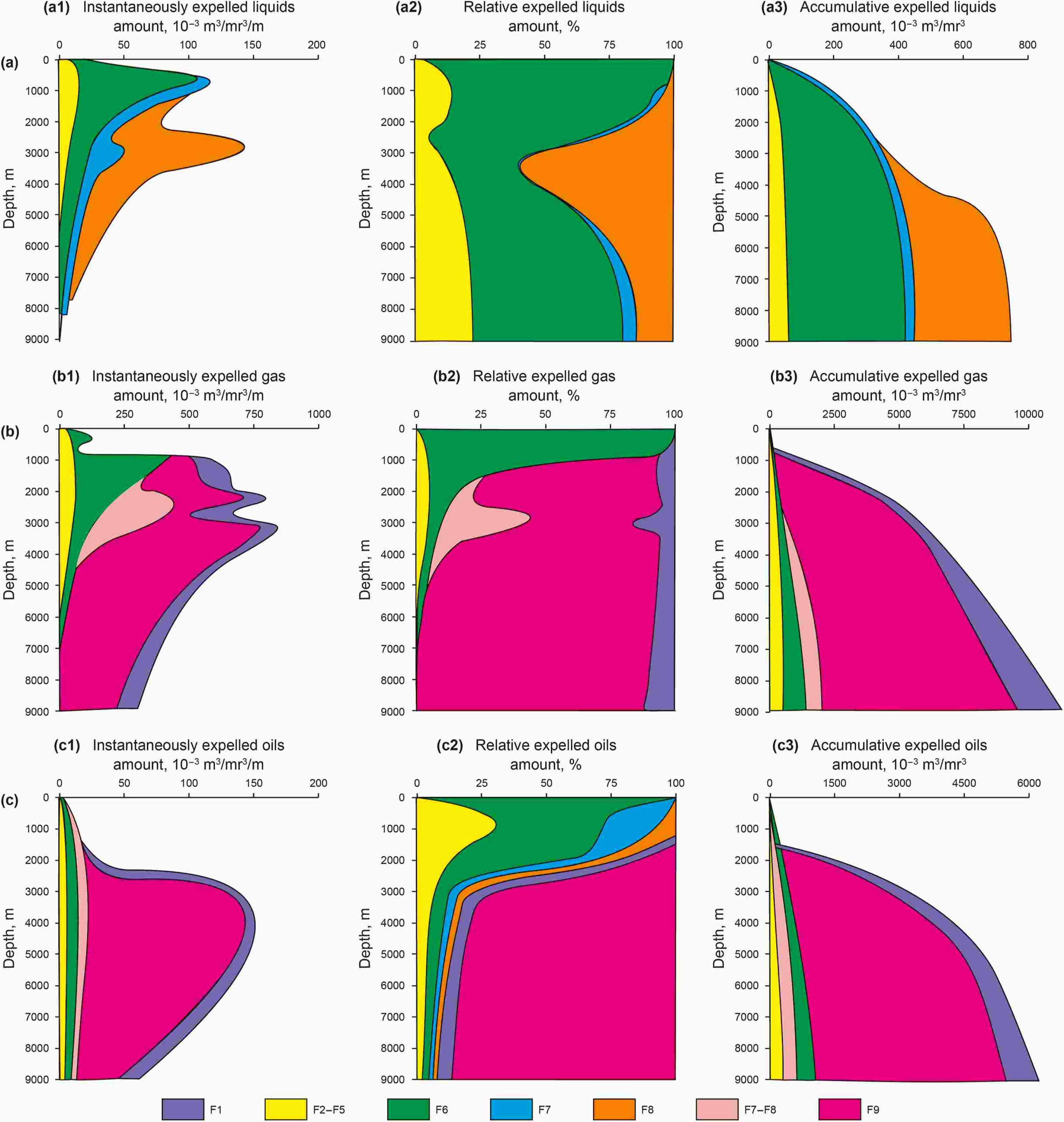

(a1) Instantaneously expelled liquids amount, 10^{-3} m³/mr³/m
(a2) Relative expelled liquids amount, %
(a3) Accumulative expelled liquids amount, 10^{-3} m³/mr³
(b1) Instantaneously expelled gas amount, 10^{-3} m³/mr³/m
(b2) Relative expelled gas amount, %
(b3) Accumulative expelled gas amount, 10^{-3} m³/mr³
(c1) Instantaneously expelled oils amount, 10^{-3} m³/mr³/m
(c2) Relative expelled oils amount, %
(c3) Accumulative expelled oils amount, 10^{-3} m³/mr³
(a)
(b)
(c)
Depth, m
0
1000
2000
3000
4000
5000
6000
7000
8000
9000
0
50
100
150
200
25
75
200
400
600
800
250
500
750
1000
2500
5000
7500
10000
1500
3000
4500
6000
F1
F2–F5
F6
F7
F8
F7–F8
F9

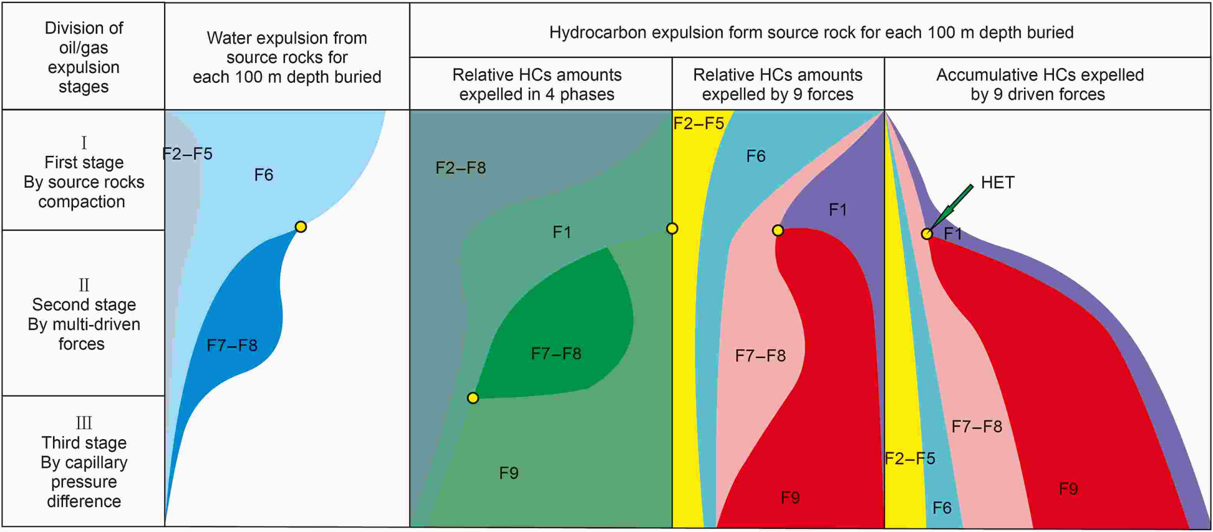
Division of oil/gas expulsion stages
Water expulsion from source rocks for each 100 m depth buried
Hydrocarbon expulsion form source rock for each 100 m depth buried
Relative HCs amounts expelled in 4 phases
Relative HCs amounts expelled by 9 forces
Accumulative HCs expelled by 9 driven forces
I
First stage
By source rocks compaction
II
Second stage
By multi-driven forces
III
Third stage
By capillary pressure difference
F2–F5
F6
F7–F8
F2–F8
F1
F7–F8
F9
F2–F5
F6
F1
F7–F8
F9
HET
F1
F7–F8
F2–F5
F6
F9

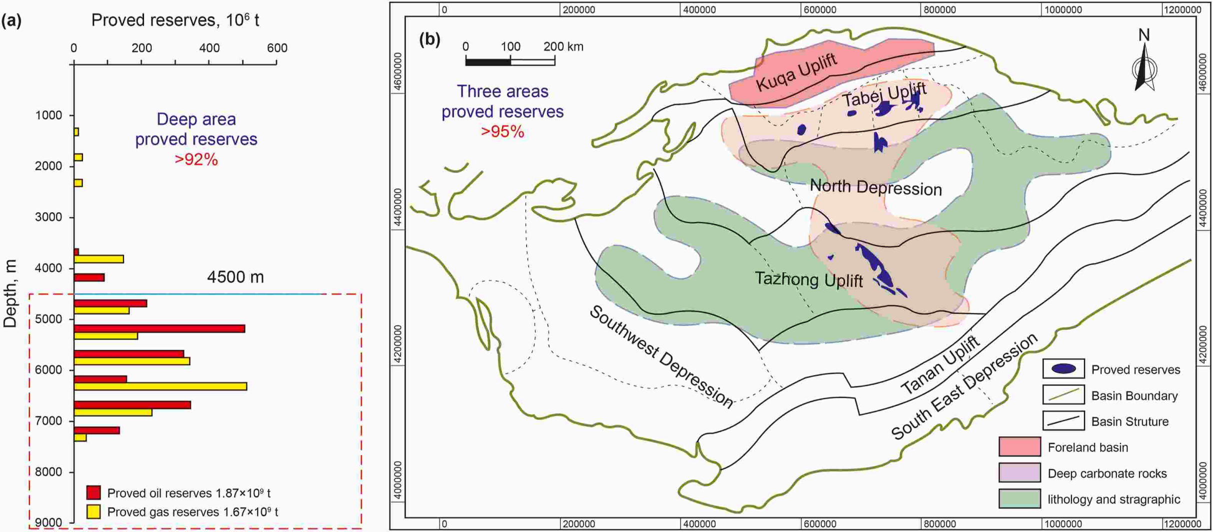
(a)
Proved reserves, 10^6 t
0
200
400
600
Depth, m
1000
2000
3000
4000
5000
6000
7000
8000
9000
Deep area
proved reserves
>92%
4500 m
Proved oil reserves 1.87×10^9 t
Proved gas reserves 1.67×10^9 t
(b)
0
100
200 km
N
Three areas
proved reserves
>95%
Kuqa Uplift
Tabei Uplift
North Depression
Tazhong Uplift
Southwest Depression
Tanan Uplift
South East Depression
Proved reserves
Basin Boundary
Basin Struture
Foreland basin
Deep carbonate rocks
lithology and stragraphic
0
200000
400000
600000
800000
1000000
1200000
4600000
4400000
4200000
4000000